Figure DR1 Kapp et al.

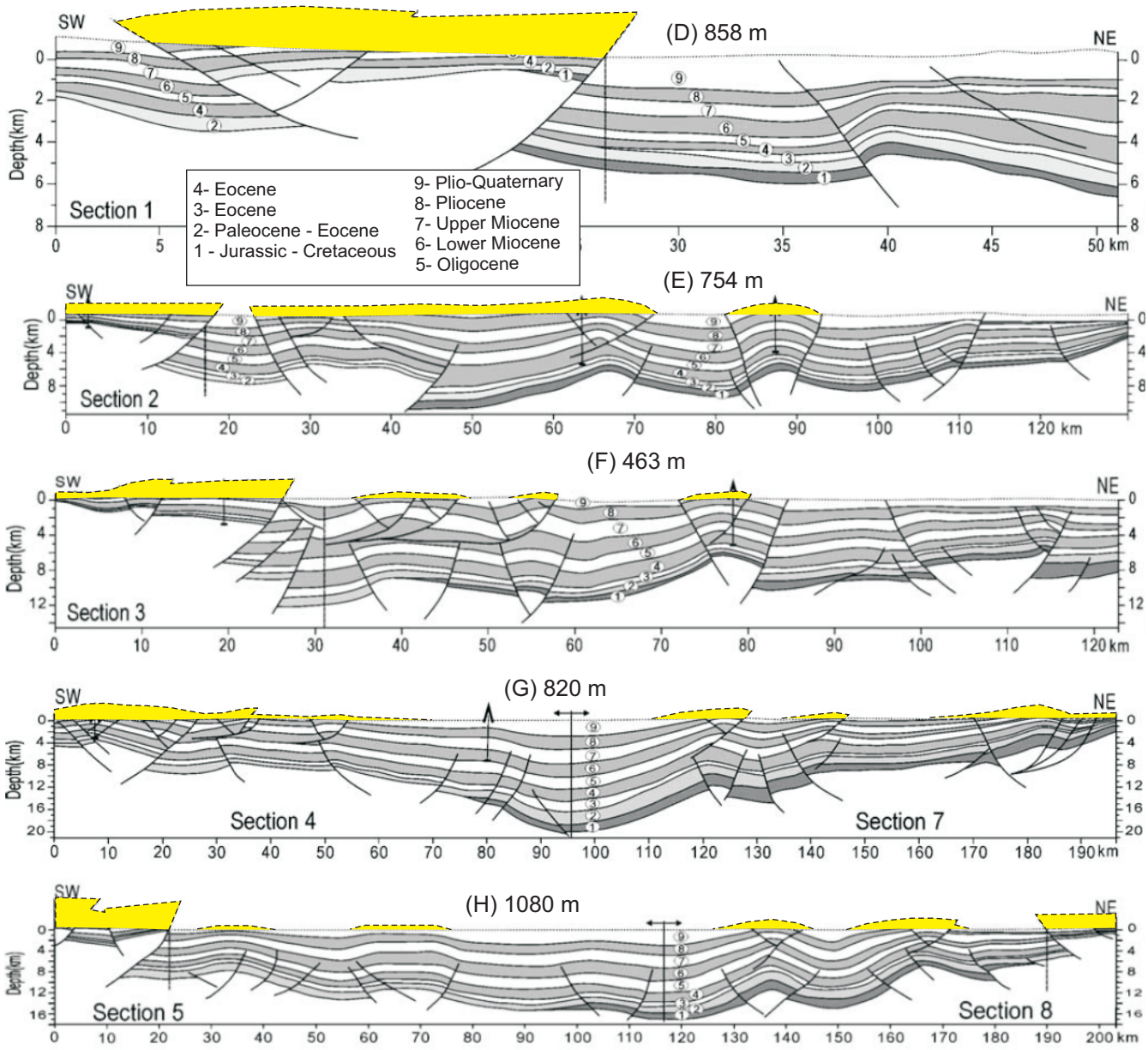

see caption next page

Figure DR1. Regional cross sections of the western Qaidam Basin constrained from seismic reflection profiles (Zhou et al., 2006). Locations of lines D-H are shown on Figure 2. Areas filled in yellow indicate the estimated amount of material eroded from above Qaidam Basin folds. The numbers in meters indicate the line-averaged value of material eroded (area shown in yellow divided by the length of the cross-section line). Erosion from above wind-eroded synclines was not taken into account. In addition, we are unable to account for the possible/likely, significant episodic wind erosion that could have contributed to thinning of the upper Pliocene and younger units.

Supplementary Note for "Wind erosion in the Qaidam Basin, central Asia: Implications for tectonics, paleoclimate, and the source of the Loess Plateau" by Kapp et al.

Model Description

Atmospheric transport of particulate matter can be modeled as a combination of turbulent diffusion, downwind advection, and gravitational settling (terms one through three, four, and five from left to right in Equation (1) below). The steady-state equation describing these processes is given by

$$\frac{\partial}{\partial x}\left(K_x \frac{\partial c}{\partial x}\right)+\frac{\partial}{\partial y}\left(K_y \frac{\partial c}{\partial y}\right)+\frac{\partial}{\partial z}\left(K_z \frac{\partial c}{\partial z}\right)-u\frac{\partial c}{\partial x}+q\frac{\partial c}{\partial z}=0\,, \qquad (1)$$

where K_x, K_y, and K_z, are the turbulent diffusivities in the x, y, and z directions, c is the particle concentration, x is the downwind distance, y is the crosswind distance, z is the vertical distance from the ground, u is the mean wind velocity, and q is the settling velocity. Solutions to Equation (1) are known as Gaussian plumes. The simplest version of the advection-diffusion-settling

equation assumes that K_z and u are uniform with distance from the ground. More sophisticated models treat K_z and u as functions of height above the ground (Huang, 1999). In this application we assume that K increases linearly with distance z above the ground (in order to model the increase in turbulent mixing as larger eddies are incorporated in the atmospheric flow at greater distances from the ground) and that u is uniform (appropriate when considering large-scale atmospheric transport, i.e. where the details of the near-surface boundary layer can be neglected). In this model framework, deposition at the ground surface is equal to the downward flux due to turbulent diffusion and particle settling. This balance provides a flux boundary condition at the ground surface ($z = 0$):

$$K_z \left.\frac{\partial c}{\partial z}\right|_{z=0} + qc(x, y, 0) = 0 . \qquad (2)$$

In this application we treat the dust from the Qaidam Basin as emanating from an elevated point source located at approximately 3000 m a.s.l. near the uppermost reaches of the Yellow River Valley (Figure 6b). The downwind deposition from an elevated point source located at $(0,0,h)$, obtained by solving (1) and (2) for the concentration at ground level downwind, is given by:

$$c(x, y,0) = \frac{Q}{hu\Gamma(1-\nu)} \exp\left(-\frac{y^2 u}{K_y x}\right) \exp\left(-\frac{h^2 u}{K_z(h) x}\right) \left(\frac{h^2 u}{K_z(h) x}\right)^{1-\nu}, \qquad (3)$$

where Q is the source emission rate and ν is the Rouse number, given by the ratio of the settling velocity and the product of the von Karman constant and the shear velocity (Huang, 1999).

Deposition over geologic time scales is accomplished by a distribution of windblown dust events of varying magnitude, duration, and orientation. In cases where detailed wind data are available over the time scales of interest, Equation (3) can be evaluated for different event conditions and integrated according to the relative frequency of those conditions. In this

application, which involves dust deposition over the entire duration of the Quaternary, detailed information about the distribution of wind conditions is not available and we must instead use mean wind conditions. Under present climates, mean wind speeds far from the ground range from 1-10 m/s worldwide (Kobayashi and Hirata, 2005). Under the glacial climates that have dominated the Quaternary, it is reasonable to assume mean wind speeds in the Loess Plateau region were at the high end of that range. Assuming a roughness length of approximately 1 mm for the Loess Plateau region (see Figure 2 of Laurent et al., 2006), a mean wind speed of 10 m/s at 10 m from the ground implies a shear velocity of approximately 0.4 m/s. Stokes' Law implies a settling velocity of approximately 5 cm/s for the median grain size (approximately 0.02 mm; Nugteren and Vandenberghe, 2004) of the Loess Plateau, thereby yielding a Rouse number of approximately 0.3. Turbulent diffusivities vary over a wide range from approximately 1 to 100 m^2/s according to the height above the ground, mean wind speed, and the stability conditions of the atmosphere (Seinfeld and Pandis, 1997). Here again we chose a value at the high end of that range (100 m^2/s) to represent $K_z(h)$, both because of the high source elevation in this case and the higher wind speeds that were prevalent during glacial climates.

Model Results

Model results are shown in Figure 4b for the reference case of u = 10 m/s, ν = 0.3, and $K_z(h) = K_x$ = 100 m^2/s. The value of the source emission rate was scaled to match the observed maximum thickness of deposits in the Loess Plateau. The basis for this scaling is the nearly equal volume of material eroded from the Qaidam Basin relative to the volume of deposits in the Loess Plateau. The source elevation was chosen to be 1500 m above the elevation of the depositional substrate, because the downwind topography of the Loess Plateau varies from 1000 to 2000 m below the source elevation of 3000 m a.s.l. (with substrate elevation decreasing with distance

downwind from the source). For dust particles fine enough to be suspended in the atmosphere (i.e. ν significantly less than 1), the model results scale with the parameter $h^2u/K_z(h)$, which has units of length. For the reference case in Figure 6b, $h^2u/K_z(h)$ = 225 km. This value represents the distance between the point source location and the distance downwind from the source where the highest dust deposition rates are predicted. The observed pattern of loess thickness (Figure 4a, modified from Nugteren and Vandenberghe, 2004), corresponds quite closely with the predicted pattern. The sensitivity of dust deposition patterns corresponding to different values of u and $K_z(h)$ can be determined by calculating $h^2u/K_z(h)$ and stretching or contracting the downwind deposition patterns linearly relative to the reference case value of 225 km. For a range of reasonable u and $K_z(h)$ values (i.e. u = 5-15 m/s, $K_z(h)$ = 50-150 m^2/s), the downwind distance of the deposition "hotspot" varies within a range of 75 to 675 km. These results support the hypothesis of a localized western source for the majority of the Loess Plateau deposits. If the value of K_y in the model is assumed to be equal to K_x, a relatively narrow plume is predicted, however. The width of the actual plume in the crosswind (N-S) direction is most likely controlled not by K_y, but by the variation in wind direction from pure westerly winds. In the results of Figure 6b, the effect of variable wind direction was represented approximately by increasing the value of K_y to a value of $2x10^5$ m^2/s in order to match the observed plume width.

The model does not reproduce the observed asymmetry of the thickness contours illustrated in Figure 4a. This asymmetry may be associated with a N-S gradient in wind velocity and/or secondary dust sources from the north. Figure 4c illustrates the model thickness contours corresponding to a case with a N-S wind velocity gradient included in the model. The effects of a N-S wind velocity gradient (i.e. higher wind speeds in the northern Loess Plateau relative to the south) are included in the model by imposing a linear N-S gradient in u in Equation (3). This

version of the model reproduces the asymmetry of the plume and hence provides one possible explanation for that asymmetry. Higher wind velocities in the northern Loess Plateau are also consistent with slightly coarser textures observed there (60-70% > 0.016 mm) relative to the southern Loess Plateau (40-50% > 0.016 mm; Nugteren and Vandenberghe, 2004), since higher westerly wind speeds in the northern Loess Plateau enable coarse grains to travel farther downwind before settling out.

References

Huang, C. H., 1999, On solutions of the diffusion-deposition equation for point sources in turbulent shear flow: Journal of Applied Meteorology, v. 38, p. 250-254.

Kobayashi, Y., and Hirata, M., 2005, Estimation of wind resources throughout the world: Heat Transfer – Asian Research, v. 34, p. 279-292.

Laurent, B., Marticorena, B., Bergamettim, G. and Mei, F., 2006, Modeling mineral dust emissions from Chinese and Mongolian Deserts: Global and Planetary Change, v. 52, p. 121-141.

Nugteren, G. and Vandenberghe, J., 2004, Spatial climatic variability on the Central Loess Plateau as recorded by grain size for the last 250 kyr: Global and Planetary Change, v. 41, p. 185-206.

Seinfeld, J.H. and Pandis, J.H., 1997, Atmospheric Chemistry and Physics: From Air Polution to Climate Change: Wiley-Interscience, New York.